International Journal of Machine Tools & Manufacture 211 (2025) 104320

Contents lists available at ScienceDirect

International Journal of Machine Tools and Manufacture

journal homepage: www.elsevier.com/locate/ijmactool

Short Communication

Derivation of physical equations for high-speed laser welding using large language models

Kyubok Lee [a,1], Zhengxiao Yu [a,1], Zen-Hao Lai [b], Peihao Geng [a], Teresa J. Rinker [c], Changbai Tan [c], Blair Carlson [c], Siguang Xu [d], Jingjing Li [a,b,*]

[a] Department of Industrial and Manufacturing Engineering, The Pennsylvania State University, University Park, PA, USA
[b] Department of Materials Science and Engineering, The Pennsylvania State University, University Park, PA, USA
[c] Manufacturing Systems Research Laboratory, Global Research and Development, General Motors LLC, Warren 48092, MI, USA
[d] Fuel Cell Research and Development, Global Propulsion Systems, General Motors LLC, Pontiac, MI, USA

ARTICLE INFO

Keywords:
Large language models (LLMs)
Dimensionless equation
Fluid dynamics
Humping

ABSTRACT

It is challenging to formulate complex physical phenomena that occur in a manufacturing process, particularly when the available data are limited, rendering conventional data-driven approaches ineffective. This study aims to predict humping onset in high-speed laser welding by introducing a novel framework, namely text-to-equations generative pre-trained transformer (T2EGPT). This method leverages the capabilities of large language models (LLMs), in combination with sparse experimental data and enriched literature data, to derive an interpretable and generalizable equation for predicting humping initiation. By capturing key correlations among physical parameters, T2EGPT generates a compact and dimensionless expression that accurately predicts hump formation. The equation reveals that humping arises from the interplay between inertia-driven backward melt flow and capillary-driven surface stabilization, where inertial forces drive molten metal backward and capillary forces resist surface deformation. Compared to traditional data-driven models, T2EGPT demonstrates enhanced predictive accuracy and cross-material transferability. More broadly, this study highlights the potential of LLMs to integrate textual information with data-driven discovery, enabling the extraction of physical laws in data-scarce scientific domains.

1. Introduction

Humping is a major defect in both fusion-based welding and additive manufacturing [1]. It typically arises when the welding or scanning speed surpasses a critical threshold. Humping directly limits the maximum welding speed, thereby constraining the overall productivity. Several studies have investigated the mechanisms behind humping, tracing its origins to hydrodynamic instabilities within the molten pool. Fig. 1 illustrates an example of humps in high-speed laser welding of stainless steel [2]. Surface humps form periodically at elevated speeds (Fig. 1a), and cross-sections reveal internal hump structures (Fig. 1b). At a low speed and power (0.33 m/s, 102 W), the weld surface remains smooth, however, increasing the speed to 1.42 m/s (348 W) results in distinct and periodic protrusions (Fig. 1c). In study [2], welding power was increased with welding speed to maintain full penetration. In-situ synchrotron imaging captures this transition in real time and validates the simulation results presented in Fig. 1d, which confirm rearward molten flow inside the keyhole-shaped pool, driven by recoil pressure and surface tension gradients, leading to flow instabilities and periodic solidification. A schematic of material flows is presented in Fig. 1e. Other surface defects in high-speed laser welding include underfill and spatter, which are less common compared to humping. In the current work, a text-to-equations generative pre-trained transformer (T2EGPT) framework is developed on the previous study [2], and other defects are not currently considered in this framework.

Understanding how process parameters and material properties influence the onset of humping is essential for process control. However, this remains challenging due to limited experimental and simulation data. Researchers have long sought to quantify these relationships through mathematical models. One common method combines experimental data with dimensional analysis, such as the Buckingham π theorem [3], to derive empirical relationships that normalize complex

* Corresponding author. Department of Industrial and Manufacturing Engineering, The Pennsylvania State University, University Park, PA, USA.
E-mail address: jul572@psu.edu (J. Li).
[1] These authors contributed equally: Kyubok Lee, Zhengxiao Yu.

https://doi.org/10.1016/j.ijmachtools.2025.104320
Received 20 April 2025; Received in revised form 6 August 2025; Accepted 9 August 2025
Available online 20 August 2025

variables and reveal the governing physics.

To overcome data scarcity challenges in scientific modeling, this research introduces the T2EGPT framework by leveraging the advantages of large language models (LLMs). Transformer-based LLMs, pretrained on extensive text corpora, can encode and extract a wide range of domain knowledge, including scientific principles, mathematical relationships, and contextual patterns. Their ability to operate in few-shot and zero-shot scenarios further enables them to model rare events or phenomena with minimal prior data [4], making them suitable for scientific discovery. T2EGPT integrates these strengths into a retrieval-augmented generation (RAG) system [5] combined with a rubric-based quantification mechanism. The process begins by constructing a private database, populated by literature selected through LLM-based filtering aligned with predefined topical criteria. After contextual validation, relevant publications are embedded into the database, enabling targeted information retrieval. When physical parameters relevant to humping defects in high-speed laser welding are provided, such as maximum melt velocity [6], length of the molten pool [7], thermal conductivity [7], density [8], specific heat [8], and surface tension coefficient [9], the T2EGPT framework based on the private database generates a correlation report. This report categorizes relationships by type (direct or indirect), form (linear or nonlinear), and effect (positive, negative, or negligible). These categories support a human-defined rubric employed to assess and score candidate equations generated from sparse datasets via a pattern search algorithm. The equation selected by T2EGPT demonstrates consistency with the Weber number, thereby validating the framework's effectiveness. Through this equation, the influences of material properties, peak melt velocity, and molten pool length in hump formation are discussed in detail.

2. Methods

2.1. Development of dimensionless equations

The development of dimensionless equations in this research involves two components, i.e., empirical equation development and LLMs-guided selection, as illustrated in Fig. 2. The data-driven approach, which integrates a pattern search algorithm with support vector machine (SVM) evaluation, generates candidate equations (Fig. 2a) using stainless steel data from a prior study [2] and additional data from stainless steel (SS), aluminum (Al) and titanium (Ti) alloys reported in the literature [9,10]. Meanwhile, LLMs extract descriptions of physical parameters related to humping and material flow in laser welding from the literature (Fig. 2b). The extracted descriptions produce correlation reports (Fig. 2c). An evaluation rubric, derived from these reports, is used to assess the candidate equations and identify the optimal equation with the highest T2EGPT score.

The Buckingham π theorem is applied to determine the structure of a dimensionless equation, which is expressed as,

$$\pi = q_1^{c_1} q_2^{c_2} \cdots q_i^{c_i} \tag{1}$$

where $q_1 \cdots q_i$ are i physical parameters, and the vector $\boldsymbol{c} = [c_1, \ldots, c_i]$, which defines the exponents of each physical parameter, is determined via a pattern search algorithm [11]. This process identifies the exponent c_i of each physical parameter q_i, ensuring the product $\boldsymbol{D}_{j\times i}\cdot\boldsymbol{c}$ equals the zero vector (Fig. 2a). $\boldsymbol{D}_{j\times i}$ denotes the dimensional matrix for a system with i physical parameters and j fundamental units.

Based on previous research [2], six ($i = 6$) physical parameters were identified, which are maximum melt velocity (u_{max}), length of molten pool (l), thermal conductivity (k), density (ρ), specific heat (c_p), and surface tension coefficient (γ). These parameters are characterized by four ($j = 4$) fundamental international units, i.e., length (m), time (s), mass (kg), and temperature (K). The unit contributions for each physical

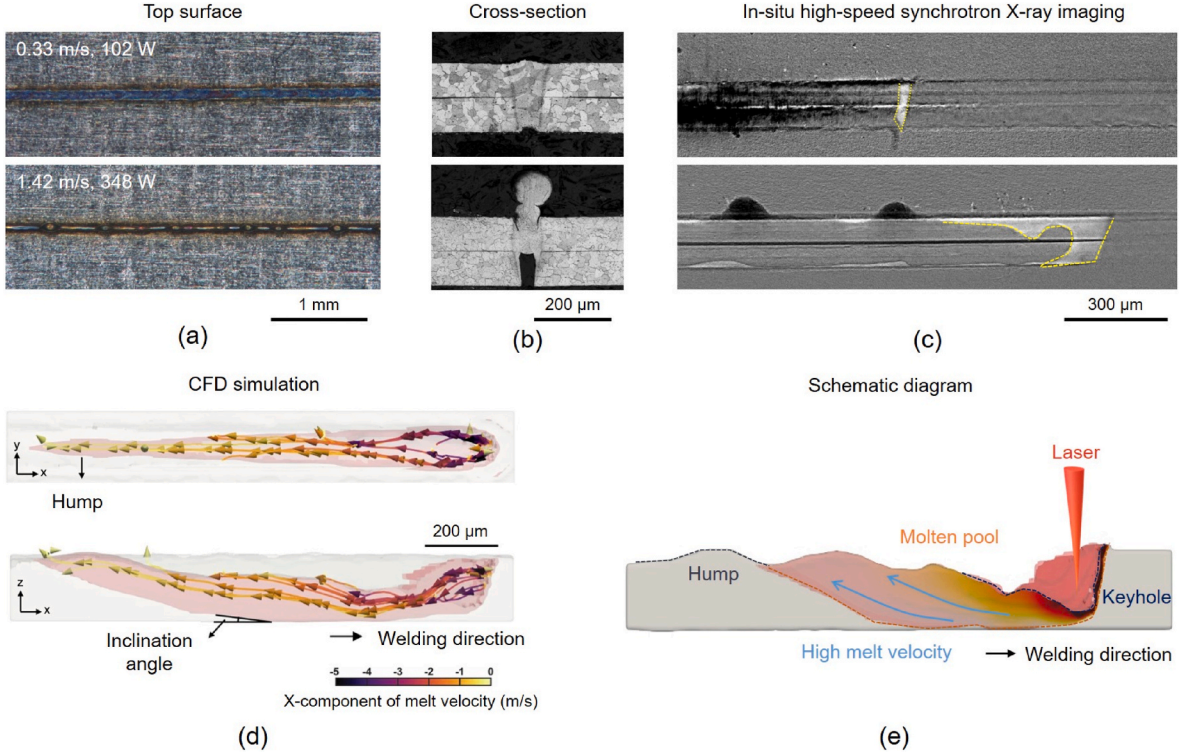

Fig. 1. (a) Top surfaces of welds without and with humps. (b) Optical microscopic images of weld cross-sections showing the absence and presence of humps. (c) No hump formation and humping observed under high-speed synchrotron x-ray imaging. (d) Top and side views of material flow during humping, as simulated using computational fluid dynamics (CFD). (e) Schematic illustration of material flow inside the molten pool during hump formation [2].

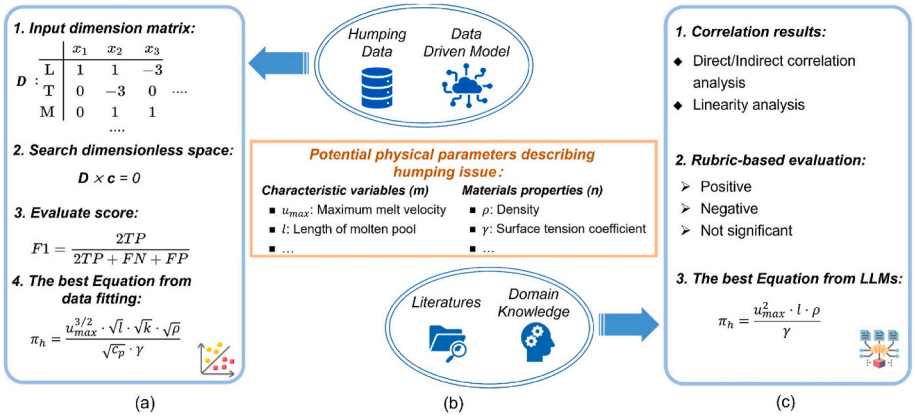

Fig. 2. Text-to-equations Generative Pre-trained Transformer (T2EGPT) overview: (a) Construction of the dimension matrix, identification of a dimensionless space, evaluation of candidate equations using the F1 score, and selection of the best equation. (b) Compilation of knowledge sources and identification of physical parameters influencing humping. (c) Analysis of candidate physical parameters, presentation of correlation outcomes, evaluation guided by structured rubrics, and equation generation using large language models (LLMs).

parameter are summarized in Table 1, forming the dimension matrix $\boldsymbol{D}_{4\times6}$. For example, for the maximum melt velocity (u_{max}), it is given by:

$$u_{max} = \frac{Length}{Time} = \frac{L}{T} \tag{2}$$

where $m = 1$ (length), $s = -1$ (time), $kg = 0$ (mass), $K = 0$ (temperature).

2.2. Development of an LLMs-based framework to evaluate candidate equations

Most literatures describe physical parameters in textual form rather than providing precise numerical equations. To integrate this qualitative knowledge into the quantitative evaluation of candidate equations, this LLMs-based framework consisits of three components:

(1) The generation of correlation reports (Fig. 2c) to identify relationships between physical parameters and the onset of humping. These reports categorize correlations into classifications such as direct, indirect, and linear or nonlinear relationships.
(2) The development of rubric-based evaluation criteria (Fig. 2c).
(3) The calculation of scores based on these rubrics to determine the best-performing equations.

2.2.1. Generation of correlation reports by LLMs

This section describes the process of generating correlation reports using LLMs. As observed in Fig. 3a, task 1 is to establish a private database. This database is pre-trained by LLMs that can retrieve humping defect-related contents. The initial search focused on literatures related to the humping defects in high-speed laser welding. The search key words were "laser welding", "humping", "melt pool geometry", "melt flow velocity", and "surface tension". The given instructions for the search process were: "Treat humping and hump as equivalent terms", "Confirm that the welding process is specifically laser welding", and "Root humping is not the same as humping; disregard any references to root humping".

In addition, LLMs were used to determine whether a literature was relevant to the humping defect. For example, the LLMs assessed a study [12] as unrelated and provided the following analysis (Fig. 3b): "The title of the paper discusses the effect of laser impingement angle on melt pool geometry and process stability during high-speed laser welding. While the paper is focused on laser welding, the abstract mentions the complete elimination of any humping in the weld profile." This indicates that this paper addresses the prevention or reduction of humping rather than exploring the formation mechanisms of humping itself.

As another example on a relevant literature [13], LLMs provided the following analysis (Fig. 3c): "The title explicitly mentions 'high-speed laser welding,' confirming that the welding process being discussed is indeed laser welding, which is a key requirement for relevance." The abstract of this paper includes the term "humping" in the context of melt flow, indicating that the paper addresses the phenomenon of humping, which is directly related to the formation mechanism being investigated. The mention of melt flow and its interdependence with the geometry of the keyhole and the melt pool suggests that this paper explores the dynamics of the welding process, which is crucial for understanding the mechanisms behind humping formation. Overall, both the title on high-speed laser welding and the discussion of humping and melt flow support that the paper is relevant.

The relevant literatures were then downloaded (Fig. 3d), and the PDF files were converted into TXT files through an embedding process. Unrelated contents, such as authorship information, affiliations, and references, were removed. Finally, a total of 100 relevant documents were stored in a private database.

As presented in Fig. 3e, task 2 involves generating a correlation report of the physical parameters. In this process, hallucination could be a potential issue in current LLMs. To mitigate potential errors (hallucinations) in LLM-generated reports, the prompt "Provide a part of the original text that supports your answer" (Appendix C, Fig. B1–3) was incorporated. This ensures that for each report (particularly those involving non-linear relationships), the LLM provides the corresponding source text, allowing researchers to incorporate domain knowledge to address incorrect outputs. Take u_{max} as an example (Fig. 3f). From the literature [13], it was found that an increase in u_{max} leads to an increase in humping formation, which is true; thus the report categorizes its impact on humping formation as "positive".

The report highlights that the correlation between u_{max} and humping formation is nonlinear. The literature indicates that this relationship is

Table 1
The dimension matrix ($\boldsymbol{D}_{4\times6}$) of physical parameters (*PV*) and fundamental units (*FU*) associated with humping defects in high-speed laser welding.

FU	*PV*					
	u_{max}	l	k	ρ	c_p	γ
Length (L)	1	1	1	−3	2	0
Time (T)	−1	0	−3	0	−2	−2
Mass (M)	0	0	1	1	0	1
Temperature (Θ)	0	0	−1	0	−1	0

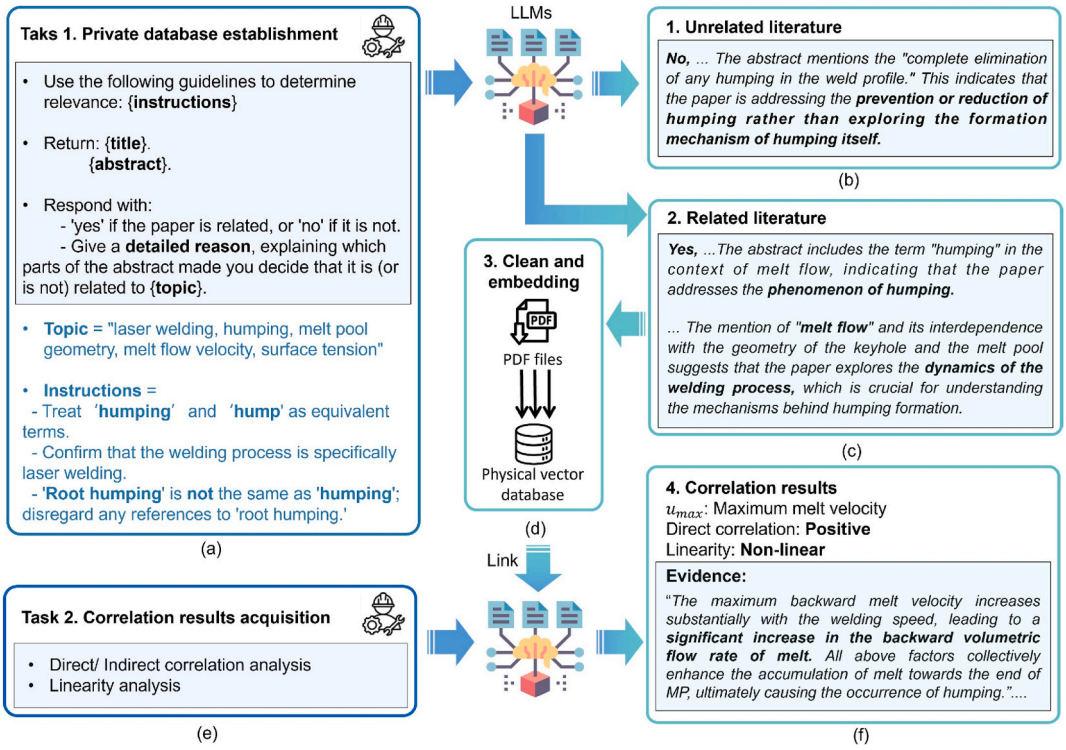

Fig. 3. Procedures in large language models (LLMs): Literature screening, database construction, and parametric correlation analysis for the humping phenomenon in laser welding. (a) Task 1: Development of a private literature database. (b) An example of unrelated literature. (c) An example of related literature, and (d) An example of private database. (e) Task 2: Generation of a correlation report between physical parameters and humping defects. (f) An example of correlation results [13].

influenced by various factors, such as welding speed, laser power, and melt pool dynamics, which do not exhibit a simple linear relationship. As the laser welding speed increases, u_{max} rises significantly. The melt flow velocity exhibits nonlinear growth with increasing welding speed. Higher melt flow velocities lead to greater volumes of melt accumulating backward, and this accumulation is nonlinear, progressively intensifying. As a result, uneven flow rates and melt accumulation at the trailing end of the molten pool trigger the periodic formation of humping [13].

If the literature lacks evidence to establish whether the relationship between a parameter and humping onset is linear or nonlinear, the T2EGPT framework will return no supporting literatures. If the T2EGPT framework mistakenly identifies this relationship as nonlinear due to hallucinations, researchers can efficiently detect and exclude these errors based on their domain expertise.

2.2.2. *Development of rubric-based evaluation criteria and T2EGPT score calculation*

In this section, a scoring system based on rubric criteria is proposed to evaluate candidate equations (Appendix D). This rubric evaluates three key aspects, correlation, linearity, and parameter pair analyses. The rationale for selecting these criteria is detailed below:

(1) Correlation evaluates how strongly a physical parameter is related to the onset of humping.
(2) Linearity determines whether the relationship between a parameter and humping onset follows a linear trend.
(3) Parameter pair analysis reveals the effects of multiple parameters on humping onset.

By simultaneously evaluating these three aspects, T2EGPT establishes a quantitative foundation for converting qualitative insights from literature into formalized models. For example, the full scale of correlation is 20 points. If the candidate equation correctly differentiates the direct or indirect correlation of one parameter with the onset of humping, this equation earns +20 points; if the equation reflects only indirect effects, without clearly delineating the direct versus indirect influence, it receives 10 points. If the candidate equation cannot show the correlation clearly or misses the correlation, no points are awarded.

Linearity is evaluated on a 10-point scale. A candidate equation receives +10 points if it correctly identifies a linear relationship for a given parameter, represented as $c_i = \pm 1$, indicating a linear contribution of parameter i to humping onset. Misjudgments (such as identifying $c_i = \pm 1$ when the correlation report indicates a nonlinear relationship), or omissions (such as assigning $c_i = 0$ when the parameter is relevant) awarded only +5 points.

Finally, parameter pair analysis allocates up to +10 points for correctly ranking the impact of parameter pairs (i.e., maximum melt velocity (u_{max}) exerts a greater influence than the length of molten pool (l)). A correct ranking satisfies c_1 greater than c_2, with +5 points awarded if the ranking is unclear or incomplete.

Based on these three criteria, a final score is denoted as:

$$S_{T2EGPT} = \frac{1}{3} \times \left[\frac{S_{correlation}}{max(S_{correlation})} + \frac{S_{linearity}}{max(S_{linearity})} + \frac{S_{pair}}{max(S_{pair})} \right] \tag{3}$$

where $S_{correlation}$, $S_{linearity}$, and S_{pair} represent the evaluation scores for direct/indirect correlation, linearity, and the influence between parameter pairs, respectively. There are 6 parameters in this study. Two-way interaction terms are examined, resulting in 15 parameter pairs. Therefore, the maximum values of $S_{correlation}$, $S_{linearity}$, and S_{pair} are calculated as,

$$\begin{cases} max(S_{correlation}) = 6 \times 20 = 120 \\ max(S_{linearity}) = 6 \times 10 = 60 \\ max(S_{pair}) = 15 \times 10 = 150 \end{cases} \tag{4}$$

These three criteria are equally weighted in S_{T2EGPT}.

The datasets utilized to develop candidate equations are drawn from a previous study [2] and additional sources in the literature [9,10], as detailed in Supplementary Table S1. Using a pattern search algorithm (described in Appendix B), candidate equations are generated across varying dataset sizes. To manage the potential overgeneration of equations due to dataset size variation, only those with an F1 score exceeding 80% are advanced for evaluation using the T2EGPT scoring system. T2EGPT scores are not derived from the datasets themselves but are instead based on a rubric informed by correlation reports generated by LLMs. Thus, the T2EGPT evaluation is grounded in textual evidence from the literature rather than numerical data.

3. Results

3.1. Influence of dataset size and parameter weighting

Fig. 4a summarizes the rubrics and T2EGPT score formulation; and Fig. 4(b–e) lists the exponent c_i values, labeled as "index" for cases with the highest T2EGPT scores for the candidate equations fitted from the dataset size of 9, 13, 20, and 24. The larger the $|c_i|$ value indicates the greater effect of the corresponding physical parameter on the onset of humping. The relative significance of the constants varies with the dataset size. For the 9-humping dataset fitting case, c_1 (maximum melt velocity, u_{max}) demonstrates the highest positive contribution, and c_3 (thermal conductivity, k) and c_6 (surface tension coefficient, γ) exhibit negative values, indicating their negative effects on the humping. As can be observed in Fig. 4f, the T2EGPT score remains relatively high at 58.5% when the dataset size is 9. It then peaks at 60.1% when the

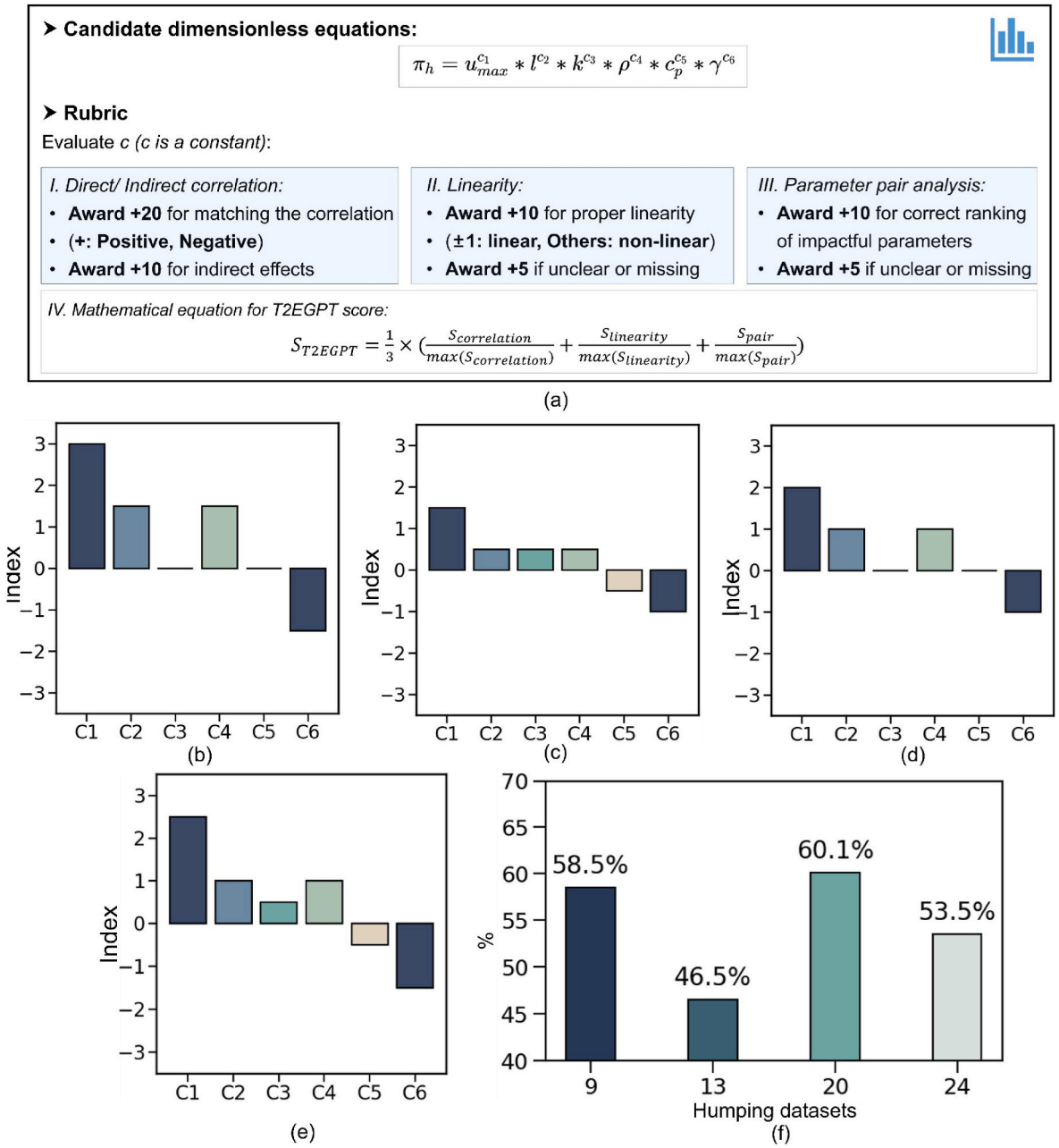

Fig. 4. Rubric of Text-to-equations Generative Pre-trained Transformer (T2EGPT) and results comparison. (a) Candidate equations and T2EGPT score formula. (b–e) Exponent c_i values fitted using datasets of sizes 9, 13, 20, and 24, respectively. (f) The final T2EGPT score of each equation based on the rubric.

dataset size reaches 20, before declining as the size increases to 24. Therefore, 20 datasets were selected for the training set.

To understand whether the rubric influences the equation evaluation, different combinations of rubrics, such as 0 points for non-compliance or missing items, are tested. The results can be found in Supplementary Table S2–S4. It is found that the trend of the final T2EGPT scores is consistent with the current rubric and the equation that achieved the highest T2EGPT score remains the same as its c_i values presented in Fig. 4d.

3.2. Validation of equations developed using the T2EGPT approach

A total of 48 datasets were used for validation in this study. These data were collected from literatures [9,10] (not included in the private database), comprising 12 datasets for aluminum alloys, 10 for titanium alloys, and 26 for stainless steels. The choice of titanium, aluminum, and stainless steel as benchmark materials reflects their distinct thermo-physical properties, enabling evaluation of model generalization across materials. For example, their melting points are approximately 934 K

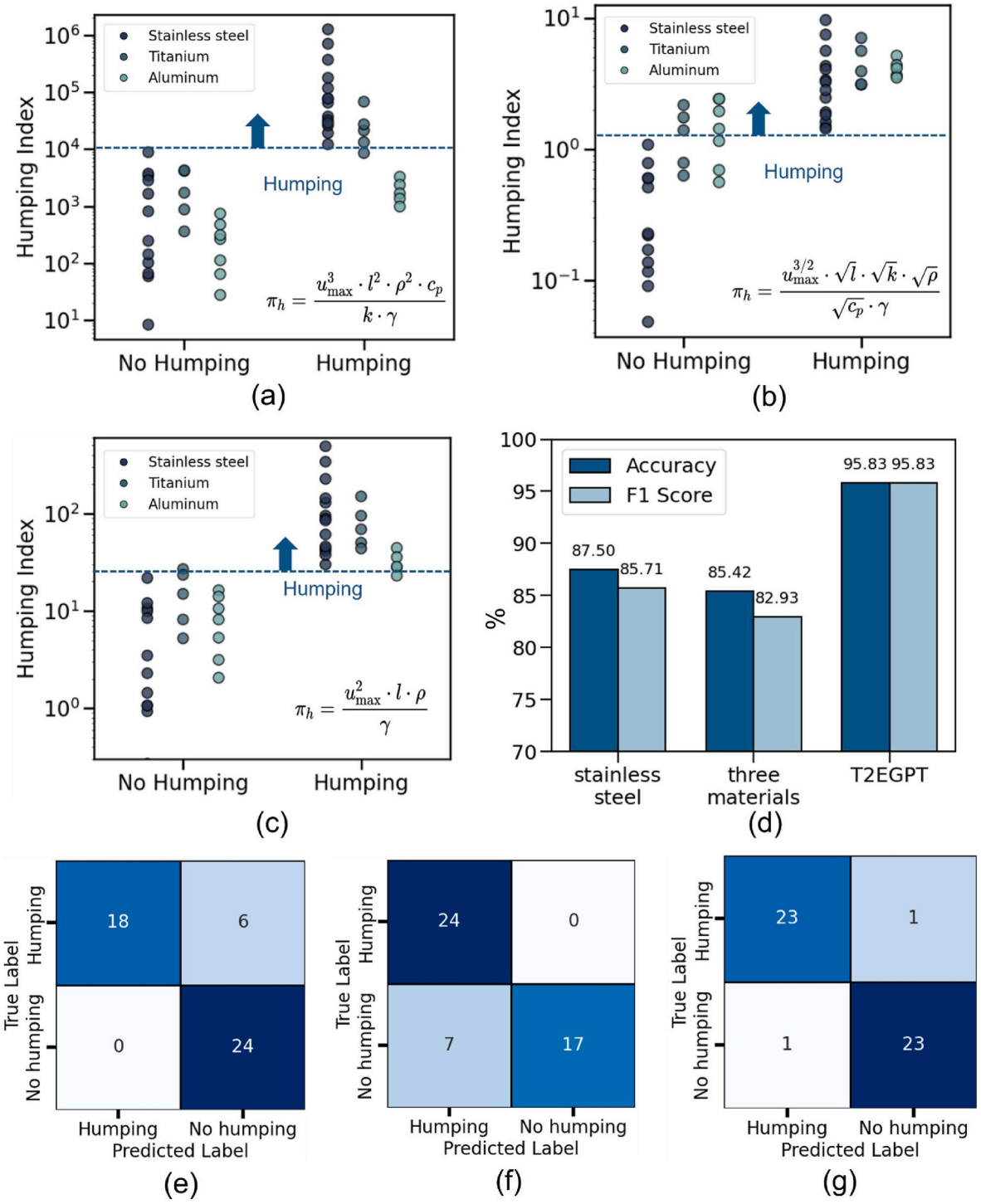

Fig. 5. Equation validations. (a) Humping index evaluated based the previous work [2], fitted with only stainless-steel data. (b) Equation fitted with 20 humping data of three materials. (c) Equation selected from text-to-equations generative pre-trained transformer (T2EGPT) framework. (d) Accuracy, F1 score (defined in Eqs. (10) and (11)), and (e–g) corresponding confusion matrices for equations (a–c).

(Al), 1944 K (Ti), and 1727 K (SS), and molten viscosities (1.3, 5.2, and 4.9 mNs/m^2, respectively). The thermophysical properties of different materials lead to distinct melt pool characteristics during laser welding. For example, aluminum's low melting point and viscosity form wider and more extended molten pools, whereas titanium's higher values for both properties lead to narrower and localized melt zones [14]. These contrasts arise from the material-dependent thermal response and flow resistance. Reduced viscosity enhances fluid mobility, leading to increased maximum melt velocities, and elevated melting points restrict the molten pool extent by demanding more thermal energy for melting [14]. Additional discussion on the detailed force interactions and velocity effects is provided through the dimensionless equation in Section 4.

Fig. 5(a–c) compares the humping index calculated using three approaches. Data points below the humping index line indicate no humping, while those above it indicates humping. Fig. 5a presents the humping index equation (Eq. (5)), as reported in a previous study [2].

$$\pi_h = \frac{u_{max}^3 \cdot l^2 \cdot \rho^2 \cdot c_p}{k \cdot \gamma} \tag{5}$$

The pattern search algorithm generated candidate equations using 20 randomly selected datasets from the literature [9,10] and a previous study [2], encompassing all three materials and remaining independent from the validation dataset. The equation (Eq. (6), shown in Fig. 5b), selected by the SVM method based on the highest F1 score (detailed in Appendix B), was validated using 48 datasets:

$$\pi_h = \frac{u_{max}^{3/2} \cdot \sqrt{l} \cdot \sqrt{k} \cdot \sqrt{\rho}}{\sqrt{c_p} \cdot \gamma} \tag{6}$$

For the T2EGPT approach, Fig. 5c presents the equation (Eq. (7)) with the highest T2EGPT score derived from the same 20 datasets.

$$\pi_h = \frac{u_{max}^2 \cdot l \cdot \rho}{\gamma} \tag{7}$$

Fig. 5d compares the accuracy and F1 scores of these three approaches on the validation dataset. For stainless steel, Eq. (5) achieves an accuracy of 87.50% and an F1 score of 85.71%; and the data-driven method on three materials (Eq. (6)) yields an accuracy of 85.42% and an F1 score of 82.93%. In contrast, T2EGPT demonstrates a significantly improved prediction on three materials data, with both an accuracy and F1 score of 95.83%. Although Eqs. (5) and (6) incorporate thermal parameters such as thermal conductivity (k) and specific heat capacity (c_p), aligning with domain knowledge of humping behavior, they underperform compared to Eq. (7) selected by T2EGPT. For instance, Eq. (5) (derived from stainless steel data) achieves 100% accuracy on the stainless steel dataset, however, exhibits reduced accuracy when applied to all three materials. Additionally, both Eqs. (5) and (6) have more complex mathematical forms with less straightforward physical interpretation, further highlighting the generalizability and physical clarity of Eq. (7).

Fig. 5(e–g) presents the confusion matrices of each candidate equation to illustrate the performance of these three approaches. T2EGPT achieves high accuracy, with only one misclassification in each category, further confirming its effectiveness in predicting humping defects.

The results demonstrate the strengths of the T2EGPT framework, which performs better than traditional data-driven approaches in predicting humping onset. Traditional data-driven approaches tend to require extensive datasets and are often optimized for individual materials. In contrast, T2EGPT exhibits robust predictive performance even with limited data inputs. Its ability to generalize across stainless steel, aluminum, and titanium alloy datasets highlights its potential as a broadly applicable and material-independent solution.

By leveraging domain knowledge with enriched textual information extracted from literature, T2EGPT identifies physically meaningful equations that capture the influence of key variables on humping onset. This flexibility is crucial for industrial manufacturing, where welding and other fabrication processes often involve diverse materials and varying process conditions.

The T2EGPT framework is not restricted to specific input formats or datasets, making it broadly applicable to other fields involving dimensionless physical equation discovery. By adjusting the search keywords and focusing on appropriate physical parameters, this framework can be effectively extended beyond welding processes. It is believed that this T2EGPT framework can alleviate the challenges faced by data-driven methods, including the scarcity of critical physical parameters and limitations in model generalization.

4. Discussion

The dimensionless humping index (Eq. (7)) derived by the T2EGPT framework exhibits the same mathematical form as the Weber number ($We = \rho v^2 l/\gamma$, where v is fluid flow velocity), which is often used to analyze fluid flows at fluid-fluid or fluid-gas interfaces. In high-speed laser welding, this equation captures the balance between inertia-driven backward melt flow and capillary-driven surface stabilization. The inertia term ($F_{inertia}$) is characterized by the dynamic pressure scale, $F_{inertia} \sim \rho u_{max}^2$, where ρ is the molten metal density and u_{max} is the maximum melt velocity. This term characterizes the fluid's tendency to sustain backward momentum, particularly at the tail of the molten pool, where metal accumulation can trigger interfacial instabilities.

In contrast, the capillary term ($F_{\text{capillary}}$) arises from surface tension, which suppresses molten pool surface deformation and restores surface uniformity. It is expressed by the capillary pressure scale, $F_{\text{capillary}} \sim \gamma/l$, where γ is the surface tension coefficient and l is the characteristic length, typically the molten pool or the gouging region length [7]. This study adopts the molten pool length as it more effectively captures the humping phenomenon, which occurs at the trailing edge rather than the leading front. This capillary term represents the restorative pressure acting on a curved interface, facilitating the backfilling of molten material and mitigating surface irregularities. Therefore, the competition between inertial and capillary forces governs the onset of humping. When $F_{inertia} \gg F_{capillary}$, the surface deformation increases, leading to periodic hump formation. Conversely, when capillary force dominates, it effectively stabilizes the molten pool surface against flow-driven disturbances.

Both Eqs. (5) and (6) identify explicit thermal transport properties such as thermal diffusivity, $\alpha = k/\rho c_p$, to represent heat transfer effect on molten pool surface deformation. Although their mathematical forms differ, both can be dimensionally reformulated into expressions relevant to combinations of the Peclet number ($Pe = vl\rho c_p/k = vl/\alpha$) and Weber number. The Peclet number characterizes the relative influence of convection versus conduction in heat transfer within the molten pool. Eq. (5) was empirically derived from previous work based on stainless steel data [2]. It is dimensionally mathematical form equivalent to $Pe \cdot We$. This formulation explicitly introduces thermal properties, aiming to account for both thermal conduction and inertial-capillary dynamics. However, due to material-dependent variability of thermal properties, the generalizability of Eq. (5) across different alloys is limited (Fig. 5e). Eq. (6), on the other hand, was obtained through a data-driven approach trained on a mixed dataset comprising different alloys. This equation can be dimensionally equivalent in mathematical form to $Pe^{-0.5} \cdot We$. It implies that the algorithm automatically down weighted the role of thermal transport, instead placing greater emphasis on inertial-capillary interactions.

Because both the Peclet and Weber numbers account for thermal transport effects and share several physical parameters, such as the u_{max} and l, they are not fully independent and may exhibit partial correlation. Consequently, determining whether to include both the Peclet and Weber numbers in an equation, or just one, can be challenging, especially when constrained by limited datasets and domain knowledge. The

application of the T2EGPT framework identifies the Weber number as the most effective descriptor of humping onset. This suggests that the influence of the Peclet number is implicitly accounted for by other dimensionless variables within the humping index (Eq. (7)), such as the molten pool length and maximum melt velocity.

Providing a real-time prediction framework for laser welding process is critical for industrial applications. Recent studies have demonstrated the effectiveness of real-time defect prediction using deep learning models [15] and infrared thermography combined with SVM classification [16]. These approaches are highly sensitive to defects such as porosity and keyhole instability and are primarily data-driven and sensor-dependent. The T2EGPT framework provides a physics-informed alternative, leveraging domain-specific knowledge to generate interpretable equations. These equations not only serve as post hoc explanations but also offer actionable insights for process design (by identifying critical thresholds of melt-flow velocity, recoil pressure, or keyhole aspect ratio, which govern the onset of porosity or humping).

A promising direction for future is integrating of T2EGPT with real-time sensing data. For example, real-time data from high-speed optical imaging of weld pool surface geometry [15] or infrared thermography [16] can dynamically evaluate the physics-based equations generated by T2EGPT, enabling adaptive and interpretable control. Such a hybrid approach can reduce reliance on large training datasets and enhance model transferability across diverse welding configurations.

5. Conclusions

In this study, a novel framework, text-to-equations generative pre-trained transformer (T2EGPT) is introduced, which combines large language models (LLMs) with rubric-based evaluation to derive interpretable and generalizable the dimensionless equation for predicting humping onset in high-speed laser welding. This framework effectively bridges the gap between sparse data and physical interpretation by transforming literature-derived knowledge into quantitative equations. The main conclusions are as follows:

1) According to the predictions of the T2EGPT framework, humping formation is attrubuted to the imbalance between inertia-dominated melt flow and surface stabilization governed by capillary forces. This result was supported by the Weber number.
2) The framework demonstrates high prediction accuracy and transferability across stainless steel, aluminum, and titanium alloys, addressing the limitations of traditional data-driven approaches under limited data conditions.
3) By leveraging LLM-extracted knowledge and rubric-guided evaluation, T2EGPT enables accurate numerical representation of defect mechanisms without relying on large datasets. Its methodology offers a scalable and interpretable alternative to black-box models and can be extended to other data-scarce physical processes.
4) The physically derived equations generated by T2EGPT can be directly utilized to guide process optimization. For instance, T2EGPT identified that high maximum melt-flow velocity is a key factor in humping formation. Based on this insight, a ring-mode laser spot was implemented, which modified the melt-pool morphology, reduced melt-flow velocities, and suppressed humping defects.

Notably, the T2EGPT framework is not restricted to a specific material or weld. Its structure and outputs are inherently generalizable, making it applicable to a variety of materials, such as titanium, stainless steel, and dissimilar metal systems, as well as other laser-based processes such as additive manufacturing. This versatility positions T2EGPT as a powerful tool for understanding and optimizing complex manufacturing phenomena. By supporting interpretable models, real-time sensing, and adaptive control, the framework aligns with long-term goals in process control and innovation grounded in physical understanding.

CRediT authorship contribution statement

Kyubok Lee: Methodology, Data curation. **Zhengxiao Yu:** Writing – original draft. **Zen-Hao Lai:** Investigation. **Peihao Geng:** Writing – review & editing, Investigation. **Teresa J. Rinker:** Resources. **Changbai Tan:** Methodology. **Blair Carlson:** Resources, Project administration. **Siguang Xu:** Funding acquisition. **Jingjing Li:** Supervision, Formal analysis, Conceptualization.

Declaration of competing interest

The authors declare that they have no known competing financial interests or personal relationships that could have appeared to influence the work reported in this paper.

Acknowledgements

The authors gratefully acknowledge financial support from the U.S. Department of Energy's Office of Energy Efficiency and Renewable Energy (EERE) through the Hydrogen and Fuel Cell Technologies Office under Award Number DE-EE0009616, the U.S. National Science Foundation IUCRC Manufacturing and Materials Joining Innovation Center (Ma^2JIC) under Award Number 2052612, and the U.S. National Science Foundation CMMI under Award Number 2226976. We also appreciate Dr. Wenpeng Yin for valuable discussions. The views expressed in this work do not necessarily reflect those of the U.S. Department of Energy or the United States Government.

Appendices.

A. Private database establishment in T2EGPT

The literature search was conducted using Elsevier's API. Key search terms were carefully designed to cover relevant topics, including "humping," "laser welding," "melt pool geometry," "melt flow velocity," and "surface tension." LLM prompts were leveraged to retrieve and evaluate keyword-matched papers. To ensure the retrieved papers specifically address humping formation in high-speed laser welding, a prompt-based pipeline was implemented using the LangChain framework. A custom evaluation prompt, built with ChatPromptTemplate, guides the GPT-4o-mini model in assessing whether each paper meets the following criteria:

- Papers must address humping in the context of laser welding processes.
- Terms such as "humping" and "hump" are treated as equivalent.
- Papers discussing "root humping" are excluded, as this is outside the scope of the research.

The programming evaluated each paper's title and abstract using this structured guideline to determine its relevance. Relevant PDFs were then downloaded manually and converted to TXT format. Content extraction and cleaning were performed using LangChain's prompt-driven editing

method, which filtered out non-essential sections such as references, acknowledgments, and author information. Text from all pages was retrieved via PyPDFLoader (Fig. A). Finally, the cleaned semantic chunks were embedded using OpenAI's model and stored in a private database via the Chroma library.

```
def clean_text_with_langchain(text):
    # Step 1: Find relevant text based on the instruction
    prompt = PromptTemplate.from_template(
    """
    You are a specialist in editing documents.
    Your task is to correct errors in the document without reducing or altering the original content.

    Remove
    * Unnecessary parts (references, acknowledgments, author lists, and keywords),
    but always keep the main contexts.

    Correct
    * Errors caused by PDF parsing, including 1. fragmented or split sentences, and
    2. incorrectly formatted or incomplete equations.

    Add
    * 'Title:' before the title of the paper.

    Document: {text}
    """
    )
```

Fig. A. Prompt template used for extracting and cleaning relevant text from literature.

B. Generation and selection of candidate equations

A pattern search method [11] was used to identify candidate $\boldsymbol{c}$ values.

$$\pi_h = u_{max}^{c_1} * l^{c_2} * k^{c_3} * \rho^{c_4} * c_p^{c_5} * \gamma^{c_6} \tag{8}$$

The identified vector $\boldsymbol{c} = [c_1, c_2, c_3, c_4, c_5, c_6]$ represents the exponents of each physical parameter, meanwhile ensuring that the matrix-vector product equals the zero vector for dimensionalless constraint:

$$\boldsymbol{D}_{4\times6} \times \boldsymbol{c}_{6\times1} = [0, 0, 0, 0] \tag{9}$$

Then, a scaling matrix $\boldsymbol{D}_{4\times6} \times \boldsymbol{c}_{6\times1}$ was applied to transform the physical input data into dimensionless form, using a predefined grid with a range of $[-3, 3]$ and an interval of 0.5 for c_i.

The SVM classification [17] was used to evaluate the effectiveness of candidate dimensionless equations (denoted as π_h) in distinguishing between humping and non-humping cases. The SVM model, trained with a radial basis function (RBF) kernel, was selected for its robustness in binary classification tasks, particularly under limited data conditions. The RBF kernel offers flexibility for modeling non-linear class boundaries, and fixed hyperparameters help reduce overfitting.

In this study, the SVM acted as a binary classifier, comparing predicted labels (0: no humping, 1: humping) to ground truth (experimental data) to quantify each equation's classification accuracy.

According to the result of SVM (a decision boundary that separates the humping and non-humping cases), a threshold value (denoted as π_{h0}), was identified for humping onset. Values of π_h calculated from candidate equations below this threshold indicate the absence of humping, and values above signify the occurrence of a humping defect.

SVM evaluated multiple candidate equations from the above procedure; therefore, $F1$ score and accuracy were applied to evaluate the candidate equations.

$$F1 = \frac{2TP}{2TP + FN + FP} \tag{10}$$

where True Positive (TP), False Positive (FP), and False Negative (FN) represent correctly predicted humping samples, no humping samples mistakenly predicted as humping, and humping samples mistakenly predicted as no humping, respectively. Equations that exhibited underfitting, or non-physical behavior yielded low F1 scores were manually excluded.

In addition to the F1 score, equations were evaluated with Accuracy:

$$Accuracy = \frac{TP + TN}{TP + TN + FP + FN} \tag{11}$$

where True Negative (TN) represents correctly predicted non-humping samples.

C. Generation of correlation reports

The correlation reports were generated using a prompt-driven approach, implemented as the function _gen_corr_report. This function employed the LangChain library's PromptTemplate to structure natural language instructions, guiding the LLMs in classifying correlations based on experimental data. The function processes retrieved context (scientific literatures or experimental results) and determined whether the effect of a given parameter on humping formation is positive, negative, or neutral, as shown in Fig. B1. The function _gen_corr_report_linearity (used for prompt-based linear

analysis) leveraged the LangChain library's PromptTemplate to structure natural language instructions, as shown in Fig. B2.

```
def _gen_corr_report(self, param, retrieved_docs):
    prompt = PromptTemplate.from_template("""
    You are a scientific assistant in laser welding research,
    focused on analyzing correlations based on the provided documents.
    Answer as accurately as possible, and if the information is insufficient,
    state that the answer is unclear.

    Question: What is the effect, influence, or role of {param_description} on humping formation in laser
    Classify the correlation as "Positive," "Negative," or "Neutral" based on the following definitions:
    - **Positive**: If increasing the parameter leads to an increase in humping formation.
    - **Negative**: If increasing the parameter leads to a decrease in humping formation.
    - **Neutral**: If the parameter does not significantly affect humping formation.

    Please provide the original text you referred to for your answer.
    Retrieved documents: {context}
    Answer:
    """)

    rag_chain = prompt | self.llm | StrOutputParser()
    report = rag_chain.invoke({
        "param_description": param['description'],
        "context" : retrieved_docs
    })

    return report
```

Fig. B1. Prompt template used for evaluating the effects of parameters on humping formation.

```
def _gen_corr_report_linearity(self, param, retrieved_docs):
    prompt = PromptTemplate.from_template("""
    You are a scientific assistant in laser welding research,
    analyze the correlation based on the provided documents.
    Answer as accurately as possible, and if the information is insufficient,
    state that the answer is unclear.

    Question: What is the correlation between {param_description} and humping formation?
    Specify if the correlation is "Linear," "Non-linear," or "Unknown."
    - **Linear**: A consistent, proportional relationship between the parameter and humping formation.
    - **Non-linear**: An inconsistent or threshold-based relationship
    between the parameter and humping formation.
    - **Unknown**: Insufficient data to determine the correlation type.

    Provide a part of the original text that supports your answer.
    Context: {context}
    Answer:
    """)

    # Invoke the model to analyze the relationship
    report = prompt | self.llm | StrOutputParser()
    result = report.invoke({
        "param_description": param['description'],
        "context": retrieved_docs
    })

    return result
```

Fig. B2. Prompt template used for analyzing linearity of parameter effects on humping formation.

The instruction for parameter pair analysis was provided in Fig. B3, where {param_list} comprises six (i) physical parameters, including maximum melt velocity (u_{max}), length of molten pool (l), thermal conductivity (k), density (ρ), specific heat (c_p), and surface tension coefficient (γ). Meanwhile, {context} refers to the relevant description in the private database document.

```
def _gen_corr_report_multi_params(self, params, retrieved_doc):
    prompt = PromptTemplate.from_template("""
    You are a scientific assistant in laser welding research.
    Based on the provided documents, analyze the correlations among the variables.
    Answer as precisely as possible, and if information is insufficient,
    state that the answer is unclear.
    Focus specifically on ranking the relative importance
    of variables in influencing humping formation.

    Question: Rank the following variables in terms of
    their relative impact on humping formation: {param_list}.
    Assess how the interaction between each pair of variables contributes to humping formation.

    Provide relevant excerpts from the original text to support your answer.
    Context: {context}

    Answer:
    """)

    # Invoking the model to generate the report
    report = prompt | self.llm | StrOutputParser()
    result = report.invoke({
        "param_list": params,
        "context": retrieved_doc
    })

    return result
```

Fig. B3. Prompt template used for ranking multi-parameter effects on humping formation.

D. Rubric in T2EGPT

The rubric in T2EGPT evaluates candidate equations based on three criteria: correlation, linearity, and parameter pair impact, as described below:
Correlation (20 points):

- The full score for correctly identifying correlations is 20 points.
- If the candidate equation correctly identifies the correlation direction, it earns +20 points for direct correlations.
- If the equation identifies an indirect effect, it earns +10 points.
- If the equation fails to show or misses the correlation, 0 points are awarded.

Linearity (10 points):

- The full score for linearity is 10 points.
- +10 points are awarded when the equation correctly captures linear relationships.
- If the equation has ambiguous or incomplete linearity assessments, +5 points are given.

Parameter Pair Impact (each pair 10 points):

- For analyzing parameter pairs, the full score of each pair is +10 points.
- If the candidate equation correctly ranks the impact of parameter pairs, it earns +10 points.
- If the ranking is unclear or incomplete, only +5 points are awarded.

A rubric based on subjective design is not a new approach and has been used in current LLMs research to evaluate the textual information [18,19]. Although the design of rubric is subjective, it still demonstrates a better effectiveness and efficiency to achieve systematic and reproducible evaluation compared to cases without rubrics [20]. Weights in the rubrics were selected to reflect the relative importance of each reasoning element in the context of domain knowledge. Correlation is considered the most important rubric, followed by linearity and the impact of individual parameter pairs in order of importance.

Correlation is assigned the highest weight, 20 out of a total 50 points, as it represents the interaction between variables that must be identified first when formulating an equation. Misinterpreting these correlations can result in T2EGPT generating equations that lack physical validity.

Linearity receives a weight (10 points), allowing the rubric to capture how each parameter influences the humping defect in a proportional way.

Parameter pair impact is assigned a weight of 10 points per pair to assess the relative importance of interactions between multiple variables.

This structure enhances the robustness of the evaluation by penalizing critical omissions (e.g., awarding 0 points for missed correlations).

To further confirm that the manually designed rubric does not influence the final equation outputs, various combinations of rubric schemes were tested (presented in Supplementary Table S2–S4). The results indicate that these different configurations (such as modifying the score for "Fails to show correlation" from 0 points to −10 points) do not affect the final equations inferred by T2EGPT.

E. T2EGPT-assisted novel laser welding process

The formation mechanisms of humping in high-speed laser welding were investigated through computational fluid dynamics (CFD) simulations, as illustrated in Fig. Ea. The molten pool morphology and maximum melt velocity were obtained from simulations under varying welding speeds. As welding speed increases, a pronounced backward melt flow emerges, which gradually traverses the entire molten pool without sufficient deceleration. The simulations reveal that u_{max} increases with welding speed and power as shown in Table E. With increasing welding speed, the keyhole becomes more elongated [2]. This change reduces the geometrical constraint on the backward melt flow, allowing for higher momentum accumulation toward the molten pool tail. These insights are corroborated by the in situ high-speed synchrotron X-ray imaging shown in Fig. Eb, which compares the keyhole morphology under non-humping (0.33 m/s, 102 W) and humping (1.42 m/s, 348 W) conditions. At the lower welding speed, the keyhole rear wall remains relatively shallow, and the molten pool is compact, promoting gradual deceleration of the backward melt [2].

Table E
Simulation results of maximum melt velocity (u_{max}) under two different welding speed and power conditions [2]

Speed, Power	u_{max} (m^3/s)
0.33 m/s, 102 W	0.92
1.42 m/s, 348 W	5.69

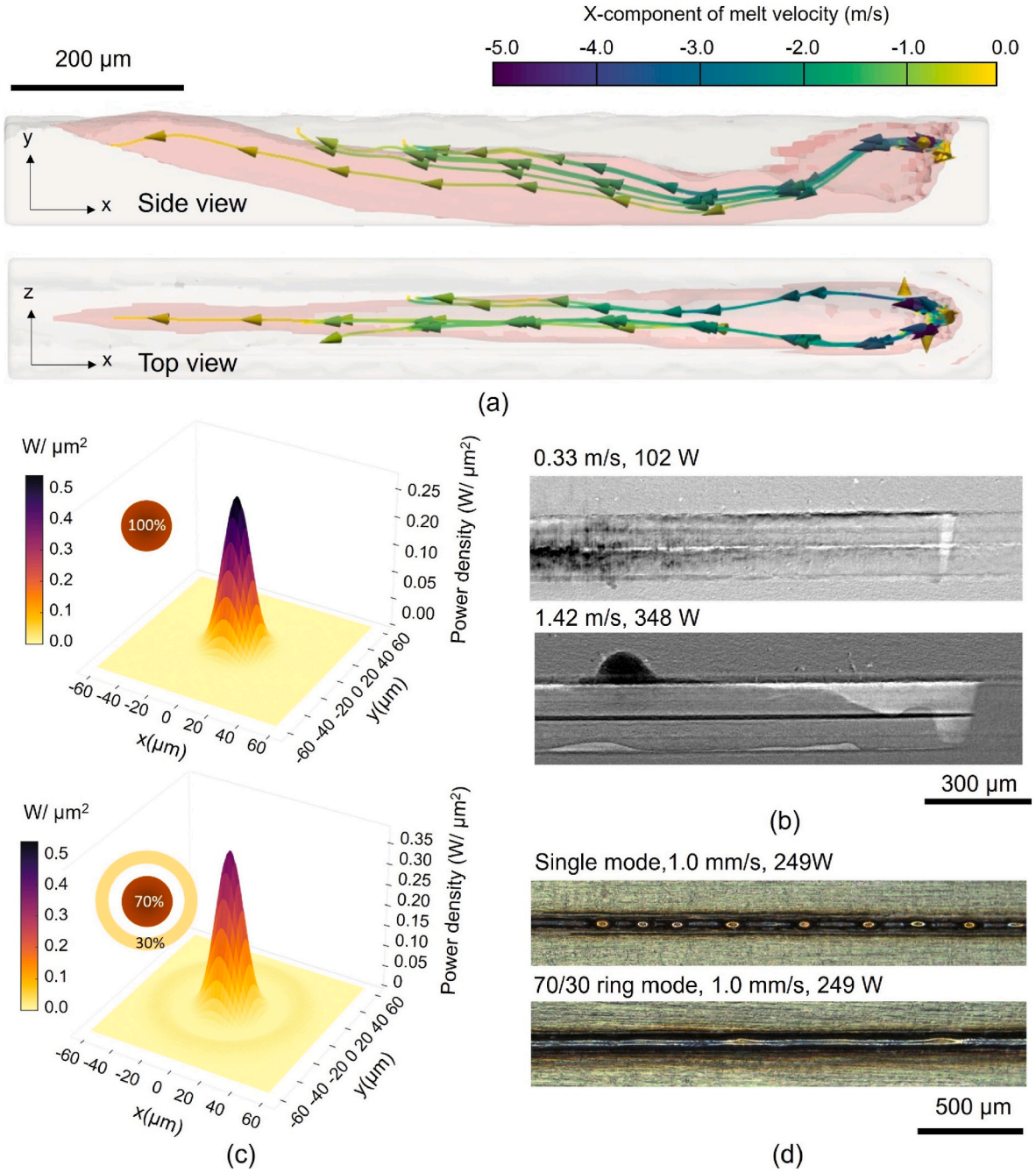

Fig. E. (a) Simulated molten pool morphology and corresponding maximum melt velocity distribution. (b) Keyhole shapes observed under high-speed synchrotron X-ray imaging for non-humping (welding speed: 0.33 m/s, power: 102 W) and humping (welding speed: 1.42 m/s, power: 348 W) conditions [2]. (c) Comparison between ring mode (central-to-peripheral heat distribution ratio of 7:3) and single mode laser beam profiles. (d) Surface humping condition after switching to a ring mode laser beam.

The analytical dimensionless formulation derived via the T2EGPT framework (Eq. (7)) provides a physics-aware and interpretable metric to quantify the humping tendency based on fundamental process parameters. This dimensionless equation explicitly captures the effects of u_{max} to humping. The term u_{max} has the largest exponent in the dimensionless Eq. (7), indicating that it plays a significant role in determining the occurrence of humping. Under the ring mode condition, the energy density at the laser center is significantly reduced (only 70% of that in single mode). The reduction in energy density results in a lower u_{max}, as shown in Table E.

Also, the energy deposited from the outer ring primarily acts on the shoulder of the keyhole and the periphery of the melt pool, significantly influencing the local thermal environment [21]. This peripheral energy input raises the local temperature around the melt boundary, which reduces surface tension gradients. The resulting suppression of Marangoni-driven flows and associated instabilities contributes to a smoother and more stable melt pool morphology [21]. Therefore, ring mode laser can suppress the onset of humping. Fig. Ec illustrates how modifying the laser heat source profile from a conventional single-mode to a ring mode configuration (with a central-to-peripheral energy ratio of 7:3) can mitigate humping. As shown in Fig. Ed, under the same welding speed and power conditions (1.0 mm/s, 249 W), humping is reduced by the ring mode.

These observations demonstrate that the T2EGPT-generated dimensionless equation not only provides quantitative interpretability of simulation and experimental trends but also offers clues to process improvement. By minimizing the maximum melt velocity (such as ring mode laser beam),

humping tendency can be suppressed. Compared to black-box machine learning models, the transparency and physical fidelity of the T2EGPT framework allows it to be integrated directly into process optimization for welding processes.

Appendix A. Supplementary data

Supplementary data to this article can be found online at https://doi.org/10.1016/j.ijmachtools.2025.104320.

Data availability

Data will be made available on request.

References

[1] G. Soundarapandiyan, C.L.A. Leung, C. Johnston, B. Chen, R.H.U. Khan, P. McNutt, A. Bhatt, R.C. Atwood, P.D. Lee, M.E. Fitzpatrick, In situ monitoring the effects of Ti6Al4V powder oxidation during laser powder bed fusion additive manufacturing, Int J Mach Tools Manuf 190 (2023) 104049, https://doi.org/10.1016/j.ijmachtools.2023.104049.

[2] Z.-H. Lai, S. Xu, S.J. Clark, K. Fezzaa, J. Li, Unveiling mechanisms and onset threshold of humping in high-speed laser welding, Nat. Commun. 15 (2024) 9546, https://doi.org/10.1038/s41467-024-53888-w.

[3] J. Bakarji, J. Callaham, S.L. Brunton, J.N. Kutz, Dimensionally consistent learning with Buckingham Pi, Nat Comput Sci 2 (2022) 834–844, https://doi.org/10.1038/s43588-022-00355-5.

[4] P. Liu, W. Yuan, J. Fu, Z. Jiang, H. Hayashi, G. Neubig, Pre-train, prompt, and predict: a systematic survey of prompting methods in natural language processing. http://arxiv.org/abs/2107.13586, 2021.

[5] P. Lewis, E. Perez, A. Piktus, F. Petroni, V. Karpukhin, N. Goyal, H. Küttler, M. Lewis, W. Yih, T. Rocktäschel, S. Riedel, D. Kiela, Retrieval-augmented generation for knowledge-intensive NLP tasks. http://arxiv.org/abs/2005.11401, 2020.

[6] P. Yinglei, S. Jiguo, Understanding humping formation based on keyhole and molten pool behaviour during high speed laser welding of thin sheets, Eng. Res. Express 2 (2020) 025031, https://doi.org/10.1088/2631-8695/ab93aa.

[7] X. Meng, G. Qin, Z. Zou, Characterization of molten pool behavior and humping formation tendency in high-speed gas tungsten arc welding, Int. J. Heat Mass Tran. 117 (2018) 508–516, https://doi.org/10.1016/J.IJHEATMASSTRANSFER.2017.09.124.

[8] R. Liang, Y. Luo, Z. Li, The effect of humping on residual stress and distortion in high-speed laser welding using coupled CFD-FEM model, Opt. Laser Technol. 104 (2018) 201–205, https://doi.org/10.1016/j.optlastec.2018.02.024.

[9] C. Thomy, T. Seefeld, F. Vollertsen, Humping effect in welding of steel with single-mode fibre laser, Weld. World 52 (2008) 9–18, https://doi.org/10.1007/BF03266636.

[10] A. Patschger, M. Seiler, J. Bliedtner, Influencing factors on humping effect in laser welding with small aspect ratios, J. Laser Appl. 30 (2018) 032409, https://doi.org/10.2351/1.5040620.

[11] R. Hooke, T.A. Jeeves, ″Direct search″ solution of numerical and statistical problems, J. ACM 8 (1961) 212–229.

[12] M.S. Khan, S. Ali, D. Westerbaan, W. Duley, E. Biro, Y.N. Zhou, The effect of laser impingement angle on the optimization of melt pool geometry to improve process stability during high-speed laser welding of thin-gauge automotive steels, J. Manuf. Process. 78 (2022) 242–253, https://doi.org/10.1016/j.jmapro.2022.04.022.

[13] E.N. Reinheimer, P. Berger, C. Hagenlocher, R. Weber, T. Graf, Supercritical melt flow in high-speed laser welding and its interdependence with the geometry of the keyhole and the melt pool, Int. J. Adv. Des. Manuf. Technol. 131 (2024) 4253–4266, https://doi.org/10.1007/s00170-024-13266-8.

[14] B. Fotovvati, S.F. Wayne, G. Lewis, E. Asadi, A review on melt-pool characteristics in laser welding of metals, Adv. Mater. Sci. Eng. 2018 (2018) 4920718, https://doi.org/10.1155/2018/4920718.

[15] Z. Zhang, B. Li, W. Zhang, R. Lu, S. Wada, Y. Zhang, Real-time penetration state monitoring using convolutional neural network for laser welding of tailor rolled blanks, J. Manuf. Syst. 54 (2020) 348–360, https://doi.org/10.1016/j.jmsy.2020.01.006.

[16] D. Ma, P. Jiang, L. Shu, S. Geng, Real-time porosity monitoring during laser welding of aluminum alloys based on keyhole 3D morphology characteristics, J. Manuf. Syst. 65 (2022) 70–87, https://doi.org/10.1016/j.jmsy.2022.08.011.

[17] C. Cortes, V. Vapnik, Support-vector networks, Mach. Learn. 20 (1995) 273–297, https://doi.org/10.1007/BF00994018.

[18] H. Pan, N. Mudur, W. Taranto, M. Tikhanovskaya, S. Venugopalan, Y. Bahri, M. P. Brenner, E.-A. Kim, Quantum many-body physics calculations with large language models, Commun. Phys. 8 (2025) 49, https://doi.org/10.1038/s42005-025-01956-y.

[19] S.A. Reji, R. Sheik, S. A, A.R. M, S.J. Nirmala, Enhancing LLM performance on legal textual entailment with few-shot CoT-based RAG, in: 2024 IEEE International Conference on Signal Processing, Informatics, Communication and Energy Systems (SPICES), 2024, pp. 1–6, https://doi.org/10.1109/SPICES62143.2024.10779705.

[20] A. Pathak, R. Gandhi, V. Uttam, Devansh, Y. Nakka, A.R. Jindal, P. Ghosh, A. Ramamoorthy, S. Verma, A. Mittal, A. Ased, C. Khatri, J.S. Challa, D. Kumar, Rubric is all you need: enhancing LLM-based code evaluation with question-specific rubrics. http://arxiv.org/abs/2503.23989, 2025.

[21] L. Wang, M. Yao, X. Gao, F. Kong, J. Tang, M. Jun Kim, Keyhole stability and surface quality during novel adjustable-ring mode laser (ARM) welding of aluminum alloy, Opt. Laser Technol. 161 (2023) 109202, https://doi.org/10.1016/j.optlastec.2023.109202.